Pis'ma v ZhETF, vol. 82, iss. 9, pp. 682 – 687

Irreversible electronic transition with possible metallization in $Y_3Fe_5O_{12}$ at high pressure

A. G. Gavriliuk[+*∇], *V. V. Struzhkin*[*], *I. S. Lyubutin*[∇1)], *I. A. Trojan*[*]

[+]*Geophysical Laboratory, Carnegie Institution of Washington, 5251 Broad Branch Road NW, Washington, DC 20015*

[*]*Institute for High Pressure Physics RAS, 142190 Troitsk, Moscow region, Russia*

[∇]*Institute of Crystallography RAS, 119333 Moscow, Russia*

Submitted 27 September 2005

The effect of high pressure up to 70 GPa on the optical absorption spectra in yttrium iron garnet $Y_3Fe_5O_{12}$ single crystals was studied in diamond anvil cells. In the pressure range $40 \div 50$ GPa, an electronic transition with drastic decrease of optical gap from ~ 2.3 eV to nearly zero value was observed implying possible metallization. Final drop of the optical gap to zero is extrapolated at about 55 GPa. It is shown that the phase transition in yttrium iron garnet observed at 40–55 GPa is possibly a transition of the insulator-metal type. At decompression, back transition to insulating state is not completely reversible. Final spectrum at ambient pressure is essentially different from initial one and corresponds to the optical gap of about 1.8 eV while in the initial state the gap value is ~ 2.6 eV.

PACS: 64.60.–i, 71.30.+h, 78.20.–e, 81.40.Tv

Introduction. The yttrium iron garnet $Y_3Fe_5O_{12}$ (YIG) belongs to a well-known class of rare-earth iron garnets which are ferrimagnets with a dominant antiferromagnetic interaction [1 – 3]. It has the cubic structure with space group $O_h^{10} - Ia3d$, and the unit cell parameter is $a_0 = 12.3738$ [4]. Iron ions Fe^{3+} occupy two different sites, with octahedral and tetrahedral oxygen environments in the ratio 2:3 per formula unit, and thus build two magnetic iron sublattices with opposite directions of magnetization. Two Fe^{+3} ions from octahedral sublattice partially compensate magnetization of three Fe^{+3} ions from tetrahedral sublattice giving $5\mu_B$ of final magnetization per formula unit [1]. At ambient pressure, the Neel temperature of YIG is about 555 K.

YIG is a charge-transfer insulator with optical gap of about ~ 2.6 eV [5]. There are several d–d optical transitions in the region of transparency [5, 6]. The nature of absorption edge is charge-transfer transitions between electronic shells of Fe^{3+} ions and ligands O^{2-} [5]. It was also shown in Ref. [6] that valence of iron ions can be altered by heat-treatment in oxidizing or reducing atmospheres, or by doping with divalent or tetravalent ions, which leads to an increase in optical absorption and electrical conductivity.

In the present study, external high pressures created in diamond anvil cells were applied to the $Y_3Fe_5O_{12}$ single crystal to modify its electronic properties. The measurements of optical absorption were used to investigate parameters of electronic system.

The experiment. The high-quality $Y_3Fe_5O_{12}$ single-crystal film with thickness $\sim 7.5\,\mu$m was grown on the $Gd_3Ga_5O_{12}$ garnet substrate with the (111) direction perpendicular to the substrate, and then it was cleaved from the substrate. In an optical microscope, the crystal plate of YIG was transparent of a deep red-brown color. The YIG plate with the dimensions $\sim 60 \times 40\,\mu m^2$ was placed into a high-pressure cell with diamond anvils. Diameter of the working surface of diamonds in the cell was about $390\,\mu$m and the diameter of the hole in the rhenium gasket where the sample was placed was about $120\,\mu$m. Silicon-organic liquid PES-5 was used as a pressure medium. The pressure was determined by the standard ruby fluorescence technique. Several ruby chips with dimensions 1–5 μm were placed into the cell at different distances from the center of the hole to evaluate the pressure distribution.

The optical absorption in the near and middle IR region was measured with the help of the Fourier spectrometer "Magna-IR750" of Nicolet Company, with the spectral resolution 32 cm^{-1}. The liquid nitrogen cooled Mercury Cadmium Telluride (MCT) detector was used. Measurements in the visible and near UV regions were made with the optical system equipped with grating monochromator SpectraPro-500i, using spectral resolution about 40 cm^{-1}. The Andor Charge-Coupled Device (CCD) detector with the Peltier cooling system was used. The experimental setup used mirror optics for

1)e-mail: lyubutin@ns.crys.ras.ru

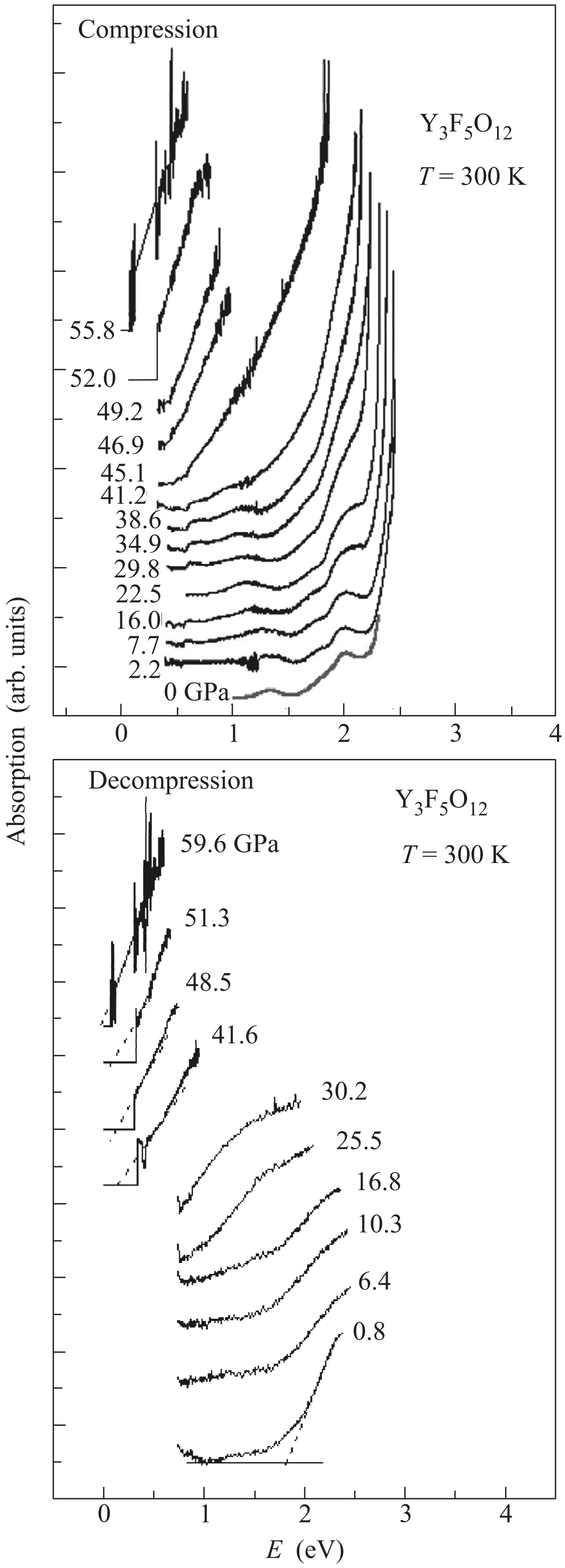

Fig.1. Evolution of optical absorption spectra in the $Y_3Fe_5O_{12}$ single crystal with pressure increase and at decompression. The spectra are recorded at room temperature

focusing the light beam on the sample and also for focusing the transmitted radiation onto the entrance slit of an optical monochromator. The diameter of the light spot on the sample surface was about 40 μm. To eliminate possible stray signals confocal pinholes were used; we measured the reference signal $\mathbf{I}_0$ outside the sample through the pressure medium and then the signal $\mathbf{I}$ transmitted through the sample. The absorption spectrum was calculated by the standard method from the formula $\mathbf{I} = \mathbf{I}_0 \cdot \exp(-\alpha \cdot d)$ where d is the sample thickness and α is the optical absorption coefficient.

Results and discussion. The room-temperature evolution of optical absorption spectra in $Y_3Fe_5O_{12}$ single crystal at pressure increase and at decompression is shown in Fig.1. The spectra exhibit rather wide absorption bands corresponding to the d–d optical transitions of the Fe^{3+} ion in the ligand crystal field. At ambient pressure before compression, the shape of the spectrum coincides with those obtained previously in [5, 6].

The sample remains transparent down to $\sim 940\,\mathrm{cm}^{-1}$ (~ 0.11 eV). Below this energy a strong lattice absorption was observed due to vibrations of the ions in the unit cell of the crystal [6]. The high-energy absorption edge is due to electronic transitions. At ambient pressure, below the absorption edge which occurs at ~ 2.6 eV, several broad absorption peaks are observed with maxima at ~ 2.0 and ~ 1.40 eV [6]. Two broad bands at ~ 1.4 and ~ 2 eV are formed by several d–d transitions of Fe^{3+} ion in octahedral and tetrahedral ligand crystal fields [5, 6]. The band at ~ 1.4 eV corresponds to the ${}^6A_{1g} \to {}^4T_{1g}$ transition of Fe^{3+} ion in octahedral sites. The second band at ~ 2 eV corresponds to the ${}^6A_1 \to {}^4T_1$ transition of Fe^{3+} ion in tetrahedral sites. We denote absorption band at ~ 1.4 eV as the **A**-band and that at ~ 2 eV as the **B**-band.

We found that during compression the energies of d–d transitions and the absorption edge linearly decrease (Fig.2) and their pressure slopes are -7.81 ± 0.43, -1.66 ± 0.22, and -8.2 ± 1.3 meV/GPa, for **A** and **B** bands, and for absorption edge, respectively. The parameters of pressure dependencies for the edge and absorption bands in YIG are presented in Table. For comparison, the analogous parameters of the $NdFeO_3$ orthoferrite where iron ions are located only in the octahedral sites are also given in Table from our recent study [7]. The comparison shows that the dE/dP values for octahedral sites in YIG and orthoferrite are close (in the limit of 30%), while for tetrahedral sites of YIG the dE/dP value is much lower.

In the pressure range from 40 to 50 GPa the absorption edge of YIG exhibits a rapid decrease from ~ 2.3

The room-temperature parameters of the optical absorption bands in the $NdFeO_3$ and $Y_3F_5O_{12}$ single crystals at ambient pressure and their pressure slopes

Transition	Energy at ambient pressure (eV)	Pressure coefficient dE/dP (meV/GPa)
$NdFeO_3$ [7]		
Edge (charge transfer)	2.42 ± 0.03	-6.94 ± 1.62
${}^6A_{1g} \to {}^4E_{1g}, {}^4A_{1g}$ (oct)	2.29 ± 0.02	-16.5 ± 0.7
${}^6A_{1g} \to {}^4T_{2g}$ (oct)	1.73 ± 0.02	-9.5 ± 0.7
${}^6A_{1g} \to {}^4T_{1g}$ (oct)	1.23 ± 0.01	-10.69 ± 0.4
$Y_3F_5O_{12}$		
Edge (charge transfer)	2.60 ± 0.03 (this study)	-8.23 ± 1.30 (this study)
${}^6A_1 \to {}^4T_1$ (tet)	2.033 [6] 2.066 ± 0.006 (this study)	-1.66 ± 0.22 (this study)
${}^6A_{1g} \to {}^4T_{1g}$ (oct)	1.40 [6] 1.40 ± 0.01 (this study)	-7.81 ± 0.43 (this study)

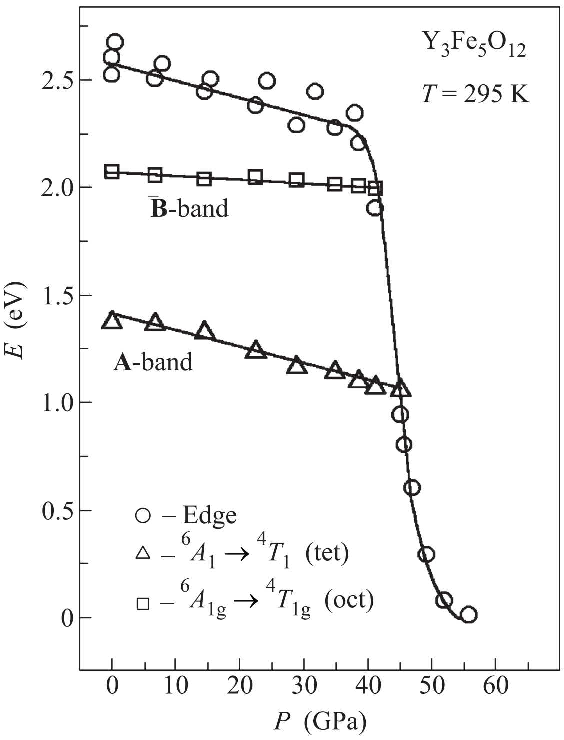

Fig.2. Pressure (P) dependence of the optical absorption edge and energies of $d-d$ transitions ${}^6A_1 \to {}^4T_2$ and ${}^6A_1 \to {}^4E$, ${}^4A$ for the pressure increase regime. Solid lines for $d-d$ transitions are linear fits

to $\sim$ 0.05 eV, which testifies the electronic transition with possible metallization. The final drop of the optical gap to zero is extrapolated to be at about 55 GPa indicating a possible complete transition to a metal state. Zero value of the optical gap we evaluated from linear extrapolation of absorption spectrum to zero intensity. At pressures higher than 55 GPa this extrapolation gave negative values of the optical gap and therefore we can conclude that above 55 GPa the complete metallization of YIG is possible.

The Fe^{3+} ion in the octahedral and tetrahedral sites does not exhibit any remarkable absorption in the visible range. Therefore, the strong absorption in oxides is attributed to the charge transfer $d^n \to d^{n+1}L$, where $n = 5$ and L is a hole in the oxygen p band [8, 9]. From the theoretical point of view, $Y_3Fe_5O_{12}$ is the strongly correlated electronic system in which, according to the Mott-Hubbard model, the gap Δ formed in the excitation spectrum due to the $O^{2-} \to Fe^{3+}$ charge transfer is smaller than the Coulomb interaction energy U [10]. For example, for octahedral clusters in the orthoferrite $LaFeO_3$, the parameters of the model determined from the X-ray and UV photoemission data are $\Delta = (2.4 \pm 0.7)$ eV and $U = (7.4 \pm 0.7)$ eV [11].

It was demonstrated in the Ref. [6] that the main contribution to intensity of **A**-band is originated from the transition ${}^6A_{1g} \to {}^2T_{1g}$ of Fe^{3+} ion in octahedral sites, while the main contribution to the intensity of the **B**-band is due to the ${}^6A_1 \to {}^2T_1$ transition of Fe^{3+} ion in tetrahedral sites. In Fig.3, the Tanabe-Sugano diagrams showing the dependence of energy terms on the crystal field is represented for Fe^{3+} ions in octahedral and tetrahedral sites. Figure 4 shows assignments of the absorption bands positions in YIG in comparison with those in the rare-earth orthoferrites (REO) and with calculation from Ref. [6]. Our comparison of the pressure behaviors of $d-d$ transitions energy in REO and YIG (see Table and Fig.3, 4) supports conclusions made in Ref. [6] that the **A**-band is due to the transition in octahedral sites while the **B**-band is due to the transition in tetrahedral sites. Using our experimental values for pressure slopes of the **A** and **B** bands energy and the

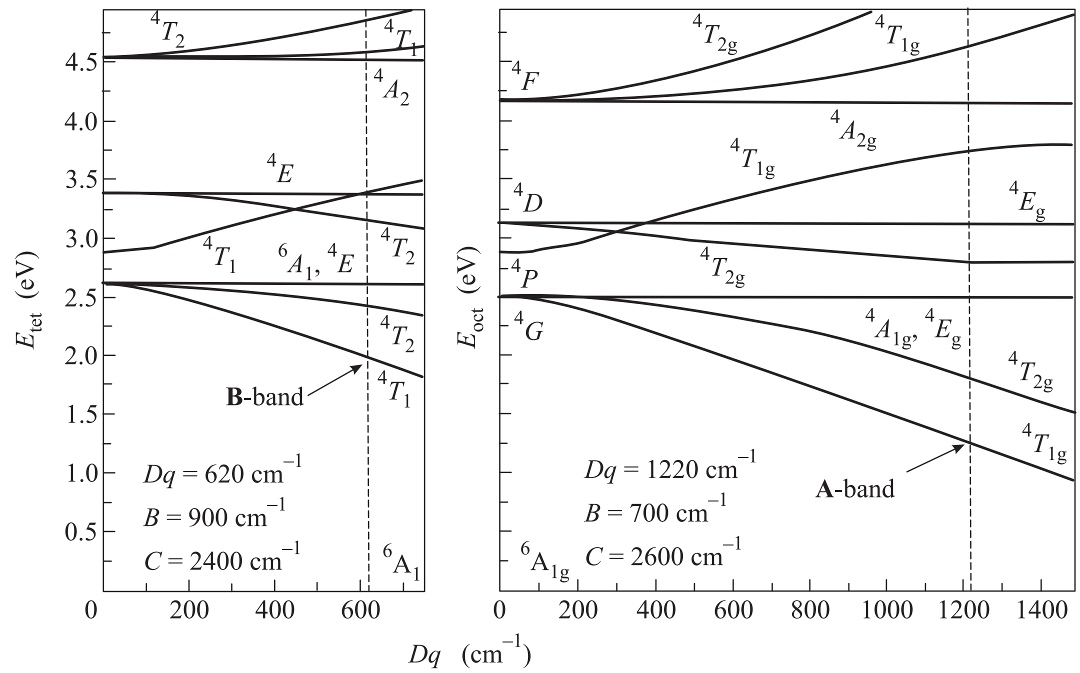

Fig.3. The Tanabe-Sugano diagram (from ref. [6]) for tetrahedral (left) and octahedral (right) environments of Fe^{3+} ion. B and C are the Racah parameters

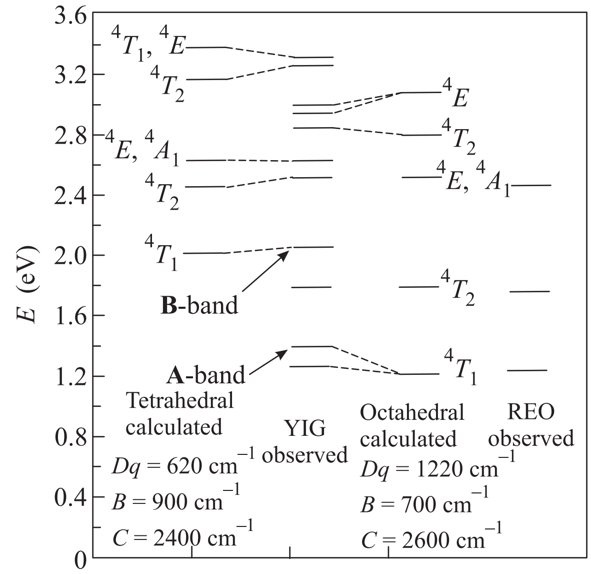

Fig.4. Assignments of the absorption bands positions in $Y_3Fe_5O_{12}$ in comparison with rare-earth orthoferrites $RFeO_3$ (REO) and with calculations from Ref. [6]. B and C are the Racah parameters

Tanabe-Sugano diagram from Ref. [6] we can evaluate the pressure slopes of crystal-field parameter for octahedral and tetrahedral sites using a simple equation:

$$\frac{d(Dq)}{dP} = \frac{1}{\partial E/\partial(Dq)}\frac{\partial E}{\partial P}. \tag{1}$$

Here $10Dq$ is the energy splitting of the term $(d^1)^2D$ in a crystal-field, and E is the energies of consequent terms in the Tanabe-Sugano diagram.

The value of $\partial E/\partial(Dq)$ can be calculated from the Tanabe-Sugano diagram at the suggestion that the Racah parameters B and C are independent of pressure. We found that these derivatives are equal to -9.2 for octahedral sites and -10.4 for tetrahedral sites of YIG. Using these values and our experimental data for $\partial E/\partial P$ (Table), finally we have:

$$\begin{aligned} \frac{\partial(Dq)_{\rm oct}}{\partial P} &\simeq +0.85\,\mathrm{meV}\cdot\mathrm{GPa}^{-1}, \\ \frac{\partial(Dq)_{\rm tet}}{\partial P} &\simeq +0.16\,\mathrm{meV}\cdot\mathrm{GPa}^{-1}. \end{aligned} \tag{2}$$

A very interesting effect was observed at the pressure decrease. We found that the observed electronic transition in YIG is irreversible. Figure 5 shows the pressure dependence of optical absorption edge both at pressure increase and at decompression. It is obvious that there is a huge hysteresis and irreversibility in behavior of the optical gap. After decompression from the high-pressure state to ambient pressure the optical gap is equal to ~ 1.8 eV, while its initial value is ~ 2.6 eV. Moreover the shape of spectrum is drastically changed from the initial one. After decompression, no absorption bands of the d–d transitions were observed. The spectral shape becomes very broad and has a tail with

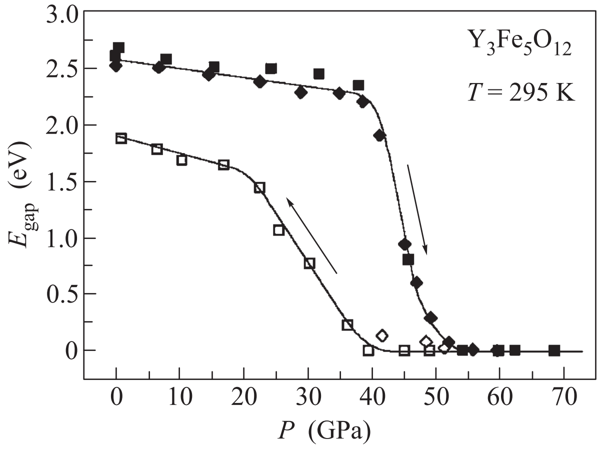

Fig.5. Pressure dependence of the optical absorption edge in $Y_3Fe_5O_{12}$ for the pressure increase (black squares and diamonds) and pressure decrease (open diamonds and squares) regimes. Two sets of symbols correspond to two sets of independent measurements. Solid line is a guide for the eye

exponential decay. A very similar behavior was observed for the amorphous YIG synthesized in Ref. [12].

Figure 6 shows the optical spectrum of our YIG after decompression to ambient pressure in comparison

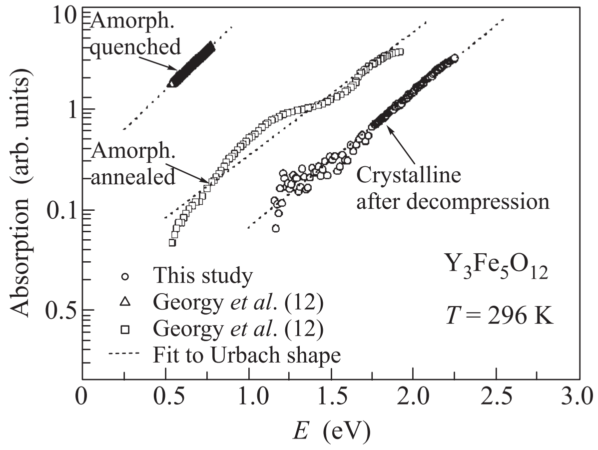

Fig.6. Optical absorption spectrum of $Y_3Fe_5O_{12}$ after decompression to ambient pressure in comparison with that from the amorphous YIG synthesized and investigated by Georgy et al. [12]. The absorption intensity (Y-coordinate) of the spectra is given in the logarithmic scale

with the spectra from the amorphous YIG synthesized and investigated by Georgy et al. [12]. The absorption intensity (Y-coordinate) of the spectra is represented in the logarithmic scale. It is obvious that after decompression the shape of absorption edge is close to exponential function $I \propto \exp(E/E_0)$ with parameter $\Gamma = 1/E_0 \sim 3.3\,\text{eV}^{-1}$. According to empirical relation for exponential Urbach-type absorption edges [13] this shape could correspond to amorphous state. For different samples of amorphous YIG [12] the parameter $\Gamma = 1/E_0$ is close to the same value ($\sim 3\,\text{eV}^{-1}$). Thus we can suggest that at the high-pressure transition in our YIG the crystal transforms irreversibly into an amorphous-like state.

The most important effect is the drastic decrease of the optical gap in the pressure range of 40–50 GPa. The decrease is not abrupt which implies an existence of some transient regime in this range of pressure when electronic correlations are suppressed and $3d$ electrons of Fe^{3+} ions are delocalizing. This effect occurs due to the transition of YIG crystal to a new, most probably metallic state. Thus, in the critical region of pressures, the YIG crystal transforms from the antiferromagnetic insulating state to most probably a paramagnetic metallic state. This transition is irreversible and accompanied by possible crystal amorphysation. Simultaneously with metallization, the transition of the iron ions from the high-spin to the low-spin state is possible, analogous to the phenomenon that was recently observed in several complex iron oxides in the pressure range of 30–50 GPa [14 – 17]. But this hypothesis needs additional experimental investigations.

An additional information about crystal structure before and after transition as well as about ions spin states and magnetic properties can be obtained from the high-pressure x-ray diffraction, Mossbauer absorption, nuclear forward scattering (NFS) and high resolution X-ray emission spectroscopy (XES) techniques. These types of experiments are in our nearest plan.

This work is supported by the DOE grant # DE-FG02-02ER45955, by the Russian Foundation for Basic Research grants # 04-02-16945-a and # 05-02-16142-a, and by the Program of Physical Branch of the Russian Academy of Sciences under the Project "Strongly correlated electronic systems".

1. Charles Kittel, *Introduction to Solid State Physics*, 4 ed., John Wiley and Sons, Inc., New York, London, Sydney, Toronto, 1971.
2. L. Neel, R. Pauthenet, and B. Dreyfus, Progress in low temperature physics **4**, 344 (1964).
3. S. Geller, J. P. Remeika, R. C. Sherwood et al., Phys. Rev. A **137**, 1034 (1965).
4. D. Rodic, M. Mitric, R. Tellgren et al., J. of Magnetism and Magnetic Materials **191**, 137 (1999).
5. A. M. Clogston, J. Appl. Phys. **31**, S198 (1960).
6. D. L. Wood and J. P. Remeika, J. Appl. Phys. **38**, 1038 (1967).

7. A. G. Gavrilyuk, I. A. Troyan, R. Boehler et al., JETP Lett. **77**, 619 (2003).
8. D. L. Wood, J. P. Remeika, and E. D. Kolb, J. Appl. Phys. **41**, 5315 (1970).
9. F. G. Kahn, P. S. Pershan, and J. P. Remeika, Phys. Rev. **186**, 891 (1969).
10. J. Zaanen, G. A. Sawatsky, and J. W. Allen, Phys. Rev. Lett. **55**, 418 (1985).
11. A. E. Bocquet, A. Fujimori, T. Mizokawa et al., Phys. Rev. B **45**, 1561 (1992).
12. E. M. Gyorgy, K. Nassau, M. Eibschutz et al., J. Appl. Phys. **50**, 2883 (1979).
13. N. F. Mott and E. A. Davis, *Electronic Processes in Non-Crystalline Materials*, Clarendon Press, Oxford, 1979.
14. A. G. Gavriliuk, I. A. Troyan, R. Boehler et al., JETP Lett. **77**, 619 (2003).
15. A. G. Gavriliuk, I. A. Trojan, I. S. Lyubutin et al., JETP **100**, 688 (2005).
16. A. G. Gavriliuk, S. A. Kharlamova, I. S. Lyubutin et al., JETP Lett. **80**, 426 (2004).
17. A. G. Gavriliuk, V. V. Struzhkin, I. S. Lyubutin et al., JETP Lett. **82**, 243 (2005).